Confidential manuscript submitted to The Geology of Iberia: A geodynamic approach. Volume 5
https://doi.org/10.1007/978-3-030-10931-8

# Slow active faults along the extensional northeastern margin of the Iberian Peninsula

**Hector Perea[1,2], Eulàlia Masana[3] and José Luis Simón[4]**

[1]GRD, Scripps Institution of Oceanography - University of California San Diego, La Jolla 92093, United States

[2]B-CSI, Institut de Ciències del Mar-CSIC, Barcelona 08003, Spain

[3]RISKNAT Group. GEOMODELS. Dep. Geodinàmica i Geofísica, Facultat de Geologia, Universitat de Barcelona, 08028 Barcelona, Spain.

[4]Dep. Ciencias de la Tierra, Universidad de Zaragoza, 50009 Zaragoza, Spain

## Introduction

The active faults located in the northeastern margin of the Iberian Peninsula are related to the extension and opening of the Valencia Trough basin. In this area, the extension began in the Neogene and two tectonic phases have been proposed (Roca, 1992, 1994, 2001, 2004; Roca and Guimerà, 1992; Roca, Roca et al., 1999; Cabrera et al., 2004): a) the rifting phase, that lasted from late Oligocene to middle Miocene, during which a rift system, with a total extension of 7.1 km, developed; and b) the thermal subsidence phase, that has been characterized by moderate tectonic activity, mainly localized at the borders of the basin, and a total extension of 4.1 km since the middle Miocene and to the present.

The northeastern margin of the Iberian Peninsula shows a range and basin morphology controlled by a horst and graben system related to the Neogene extensional faults developed during the opening of the Valencia Trough. The ranges are mainly formed by Variscan and Mesozoic rocks and the basins are filled with Neogene to Quaternary sediments. The main extensional faults are listric, dip around 60º close to the surface, show normal dip slip, accumulate kilometric displacements and may branch into a basal detachment level at 13 to 15 km (Simón, 1984; Roca, 1992, 1994, 2001; Roca and Guimerà, 1992; Tassone et al., 1994; Sàbat et al., 1995; Vidal et al., 1995; Saula et al., 1996; Roca et al., 1999; Vergés and Sabat, 1999; Gaspar-Escribano et al., 2004).

The present seismicity in the northeastern Iberian Peninsula is low to moderate, although some destructive historical earthquakes have occurred in the area (Ripoll 1152 with I=VIII; Catalan Seismic Crisis 1427 and 1428 with maximum intensities between

VIII y IX; Cardedeu 1448 with I=VIII) (Olivera et al., 2006; Perea, 2006, 2009; Perea et al., 2006, 2012). The regional stress field obtained from borehole breakout data and inversion of earthquake focal mechanisms shows minimum horizontal stress trajectories oblique to perpendicular to the main faults, favoring them remain active as extensional faults (Schindler et al., 1998; Goula et al., 1999; Herraiz et al., 2000; de Vicente et al., 2008). High-precision leveling data show the occurrence of some vertical anomalies possibly related to the tectonic activity of some of the extensional faults in the area with estimated local vertical slip-rates ranging between 0.8 and 4 mm/yr (Giménez et al., 1996; Giménez, 2001). GPS geodetic studies, focusing in the Pyrenees, suggest low regional horizontal velocities of displacement in the Catalan Coastal Ranges (0.10 to 1.09 mm/yr) with the velocity vectors slightly parallel to the main extensional faults (Asensio et al., 2012).

The following sections summarize the information about the active faults identified in the northeastern margin of the Iberian Peninsula grouped into four different geographical zones: a) the Transverse ranges, in the northeastern sector and with faults trending NW-SW; b) the Catalan Coastal Ranges, mainly composed by NE-SW trending faults, in the central part of the area; c) the Maestrat basin to the south and characterized by shorter NNE-SSW trending faults; and d) the Mediterranean sea zone with faults trending parallel to sub-parallel to the coastline. Figure 1 and Table 1 localize and synthesize the seismological parameters of each of the identified active faults.

## Active faults in the Transverse Ranges and Empordà Basin

The Transverse Ranges are a set of mountain ranges trending NW-SE bounding the Empordà Basin to the southwest. The ranges and the basin have been formed by the Neogene activity of NW-SE extensional faults (Roca, 1992; Tassone et al., 1994; Saula et al., 1996).

Within the transverse ranges, the Amer fault (nº2 in Figure 1 and Table 1) is the only fault in the area identified as a source of large historical earthquakes: the XVth century Catalan Seismic Crisis (Figure 2) (Fleta et al., 2001; Olivera et al., 2006; Perea, 2006, 2009; Perea et al., 2006, 2012). Detailed geomorphologic studies suggest two segments and Quaternary activity along the fault (Ferrer et al., 1996; Fleta et al., 2001; Perea, 2006; Perea et al., 2006). Radon gas emissions in the area show anomalies also suggesting the current activity of the fault (Font et al., 2008; Zarroca et al., 2010). To estimate its vertical slip rate it has been assumed that the height of the youngest generation of triangular facets corresponds to the minimum cumulative slip of the fault during the last 5 to 2 Ma, which yields rates between 0.05 and 0.14 mm/yr (Perea, 2006; Perea et al., 2006, 2012). In addition, this fault could generate large earthquakes with magnitudes between Mw 6.8 and 6.9 (Perea, 2006; Perea et al., 2006, 2012; García-Mayordomo et al., 2012), considering the mapped fault length as the maximum earthquake surface rupture length and using different empirical relationships (Wells and Coppersmith, 1994; Stirling, 2002; Wesnousky, 2008).

**Active faults in the Catalan Coastal Ranges**

The Catalan Coastal Ranges are composed by a set of basins and ranges trending NE-SW, sub-parallel to the coast line. They are bounded by Neogene extensional faults, being the most prominent, from northeast to southwest, the Vallès-Penedés, El Camp and Baix Ebre faults, whose activity has produced the formation of large sedimentary basins (Roca, 1992, 2001, 2004; Roca and Guimerà, 1992; Roca et al., 1999; Cabrera et al., 2004; Gaspar-Escribano et al., 2004).

The Quaternary activity of the El Camp fault (nº5 in Figure 1 and Table 1) has been demonstrated by geomorphologic and paleoseismological studies (Masana, 1995; Masana et al., 2001a, 2001b; Santanach et al., 2001, 2010; Perea et al., 2003, 2006; Perea, 2006). This fault is located in the central part of the Catalan Coastal Ranges and has a total length of about 51 km, considering that it extends on the onshore for 41 km and, at least, for 10 km into the Mediterranean Sea (Medialdea et al., 1986; Masana, 1995). Based on a geomorphologic study, the fault has been divided in four segments and along the El Hospitalet segment Masana (1995) identified a fault scarp that is offsetting alluvial fans with ages younger than 300 ka (Villamarín et al., 1999; Santanach et al., 2001). The paleoseismological analysis of eight trenches across this fault scarp have shown the repetitive occurrence of faulting events associated to earthquakes (Figure 3) and have stated that (Masana, 1995; Masana et al., 2001a, 2001b; Santanach et al., 2001, 2010; Perea et al., 2003, 2006; Perea, 2006): a) the fault has produced at least six events during the last 300 ka, three of them during the last 125 ka; b) it has a slip rate between 0.02 and 0.08 mm/yr, being the lowest value the preferred; c) it could produce a maximum magnitude earthquake up to Mw 6.7; d) the average recurrence interval between large earthquakes is 30 ka (between 25 and 50 ka); and e) the last event occurred 3000 yr ago.

The slip rates and maximum magnitudes calculated for the other segments of the fault, using the same approaches that for the Amer fault, range between 0.02 and 0.06 mm/yr and between Mw 6.2 and 7.0, respectively. The estimated slip rates are in agreement with those coming from the paleoseismological studies (Perea, 2006; Perea et al., 2006, 2012).

Other five faults located along the Catalan Coastal Ranges show geomorphic features that evidence their activity during the Quaternary (e.g. low sinuosity along the mountain fronts, presence of faceted spurs, wine-glass shape and parallel basins or convex topographical profiling across the front) (Masana, 1995; Perea, 2006; Perea et al., 2006, 2012): the Montseny, the Pla de Barcelona, the Pla de Burgar, the Baix Ebre and the Montsià faults (nº3, 4, 6, 7 and 8, respectively, in Figure 1 and Table 1). Following the same approaches explained before, the obtained slip rates range between 0.02 and 0.11 mm/yr, being the lowest slip rates for each fault the preferred ones, and the magnitudes varies between Mw 6.2 and 7.4 (Perea, 2006; Perea et al., 2006, 2012; García-Mayordomo et al., 2012).

**Active faults in the Maestrat Basin**

The Maestrat Basin is characterized by a set of NNE-SSW trending ranges and basins that extend up to 30-35 km from the Mediterranean coast and represent the southwards prolongation of the extensional faults on the Catalan Coastal Ranges into the easternmost Iberian Chain (Simón et al., 1983; Simón, 1984; Roca, 1992; Roca and Guimerà, 1992).

Several Quaternary active extensional faults have been recognized in the Maestrat Basin based on two different approaches (Simón et al., 1983, 2012, 2013; Simón, 1984; Perea, 2006; Perea et al., 2006, 2012). A first group of faults (nº12, 14, 15, 16, 19, 20, 21, 22, 23 and 24 in Figure 1 and Table 1) has been identified based on a geomorphologic and morphometric analysis of the mountain fronts related to them and by comparison to the fronts associate with the Amer and El Camp faults, proved to be active faults in the Quaternary and seismogenic (Perea, 2006; Perea et al., 2006, 2012)., The slip rates and the magnitudes of the largest earthquake they could produce have been estimated using the same approach as for the northern active faults and they range between 0.01 and 0.14 mm/yr between Mw 5.9 and 6.8, respectively (Perea, 2006; Perea et al., 2006, 2012; García-Mayordomo et al., 2012). For the Serra d'Irta and Ivarsos/Rambla de la Viuda faults (nº14 and 20 in Figure 1 and Table 1) Simón et al. (2012, 2013) have calculated slip rates ranging from 0.06 to 0.10 and from 0.12 to 0.18 mm/yr, respectively,

https://doi.org/10.1007/978-3-030-10931-8

considering the vertical offset produced by those faults in the so called *Fundamental Erosion Surface* (FES; 5.0 to 3.6 Ma). These slip rates are similar to the higher rates obtained from the height of the triangular facets (0.02 to 0.06 and 0.05 to 0.14 mm/yr), even though Perea (2006) and Perea et al. (2006, 2012) prefer the lowest values of the estimated ranges based on the comparison with the rates obtained from the paleoseismological studies on the El Camp fault.

A second group of active faults has been identified based on the fact that they offset different Plio-Quaternary deposits or surfaces (Simón, 1984; Simón et al., 2012, 2013). The Torreblanca fault (nº13 in Figure 1 and Table 1) offsets the FES and Villafranchian (2.6 to 1.9 Ma) and middle Pleistocene (253.3 ± 18.0 ka) deposits, resulting in slip rates ranging from 0.04 to 0.06 mm/yr, from 0.04 to 0.07 mm/yr and from 0.26 to 0.30 mm/yr, respectively (Simón et al., 2013). The La Vall Torta/Mas de Calduchs and Torre Endomenech/Vall d'Alba faults (nº17 and 18 in Figure 1 and Table 1) offset a mantled pediment attributed to the Villafranchian (Simón, 1984). Accordingly, the estimated vertical slip rate for both faults range between 0.02 and 0.04 mm/yr (Simón et al., 2012). In general, the slip rates calculated using the vertical offsets of deposits or surfaces are similar to those determined in close faults using the height of the triangular facets, with the exception of the middle Pleistocene rate calculated for the Torreblanca fault, which is an order of magnitude higher. The comparison of the geomorphologic features between the different mountain fronts related faults show that the mountain fronts associated with the Torreblanca, La Vall Torta/Mas de Calduchs and Torre Endomenech/Vall d'Alba faults show predominance of degradation conditions, related to very little or none active faults (Perea, 2006). Thus, the estimated long term slip rates on these three faults could be lower. The largest earthquakes that these faults could generate range between Mw 6.2 and 7.1, estimated following the same approach explained previously (Table 1).

**Active faults in the Mediterranean Sea**

The offshore margin of the northeastern Iberian Peninsula presents a wide (6 to 70 km) continental shelf with several submarine canyons dissecting the continental slope and the larger ones also the shelf. There is no surface expression of the Neogene extensional faults on the bathymetry, thus, they have been mapped by the interpretation on and correlation across a large dataset of industrial seismic reflection profiles (Roca, 1992, 1994, 2001).

On the offshore area a fault has been considered active during the Quaternary when it is offsetting the reflectors corresponding to the Plio-Quaternary sedimentary units (Perea, 2006; Perea et al., 2012). Nine faults have been classified as active: the Gulf the Roses, Western, Central and Eastern Amposta basin, Western, Central-Western, Central-Eastern and Eastern Cullera cape, and SW Columbrets basin faults (nº1, 9, 10, 11, 25, 26, 27, 28 and 29 in Figure 1 and Table 1). For these faults the vertical slip rate has been calculated measuring the offset at the base of the Plio-Quaternary formation and assuming that its age is in the time range between 5 and 2 Ma. The largest earthquake has been estimated using the same approach that for the other faults in the area. The resulting slip rates range between 0.01 to 0.10 mm/yr and the magnitudes between Mw 6.2 to 7.3 (Perea, 2006; Perea et al., 2012). However, Perea (2006) argues that the estimated slip rates are usually lower than those calculated for the onshore faults, probably because the vertical offset could have been measured in a seismic profile that it is not necessarily cutting the fault in the place of its maximum offset. Thus, this slip rates should be considered as a minimum. After the CASTOR project induced seismic sequence (September-October 2013) (Cesca et al., 2014) a specific study in the Eastern Amposta basin fault based in the analysis of multichannel seismic profiles was carried on (Fernández et al., 2014). This study better mapped the fault trace and estimated a net slip rate ranging from 0.16 to 0.26 mm/yr, an order of magnitude higher than the ones obtained previously, and a maximum magnitude earthquake between Mw 6.0 and 6.7.

## References

Asensio, E., Khazaradze, G., Echeverria, A., King, R.W., and Vilajosana, I., 2012, GPS studies of active deformation in the Pyrenees: Geophysical Journal International, v. 190, no. 2, p. 913–921, doi: 10.1111/j.1365-246X.2012.05525.x.

Cabrera, L., Roca, E., Garcés, M., and de Porta, J., 2004, Estratigrafía y evolución tectonosedimentaria oligocena superior-neógena del sector central del margen catalán (Cadena Costero-Catalana), *in* Vera, J.A. ed., Geología de España, SGE-IGME, Madrid, p. 569–572.

Cesca, S., Grigoli, F., Heimann, S., Gonzalez, A., Buforn, E., Maghsoudi, S., Blanch, E., and Dahm, T., 2014, The 2013 September-October seismic sequence offshore Spain: a case of seismicity triggered by gas injection? Geophysical Journal International, v. 198, no. 2, p. 941–953, doi: 10.1093/gji/ggu172.

de Vicente, G., Cloetingh, S., Muñoz-Martín, A., Olaiz, A., Stich, D., Vegas, R., Galindo-Zaldívar, J., and Fernández-Lozano, J., 2008, Inversion of moment tensor focal mechanisms for active stresses around the microcontinent Iberia: Tectonic implications: Tectonics, v. 27, no. 1, p. TC1009, doi: 10.1029/2006TC002093.

Fernández, F., Bohoyo, F., Maestro, A., and García-Mayordomo, J., 2014, Nuevas aportaciones sobre las características geométricas del sistema de fallas Amposta Oriental-Montsià Norte (Margen Catalano-Valenciano, España), *in* Álvarez-Gómez, J.A. and Martín-González, F. eds., Una aproximación multidisciplinar al estudio de las fallas activas, los terremotos y el riesgo sísmico. 2ª reunión ibérica sobre fallas activas y paleosismología (Lorca, Spain), IGME, p. 105–108.

Ferrer, P., Masana, E., and Santanach, P., 1996, Expresión geomorfológica de la actividad reciente de la falla de Amer (NE de la Península Ibérica): Acta Geol.Hispánica, v. 31, no. 4, p. 17–24.

Fleta, J., Santanach, P., Goula, X., Martínez, P., Grellet, B., and Masana, E., 2001, Preliminary geologic, geomorphologic and geophysical studies for the paleoseismological analysis of the Amer fault (NE Spain): Netherlands Journal of Geosciences / Geologie en Mijnbouw, v. 80, no. 3–4, p. 243–253.

Font, L., Baixeras, C., Moreno, V., and Bach, J., 2008, Soil radon levels across the Amer fault: Radiation Measurements, v. 43, p. S319–S323, doi: 10.1016/j.radmeas.2008.04.072.

García-Mayordomo, J., Insua-Arévalo, J.M., Martínez-Díaz, J.J., Jiménez-Díaz, A., Martín-Banda, R., Martín-Alfageme, S., Álvarez-Gómez, J.A., Rodríguez-Peces, M., Pérez-López, R., Rodríguez-Pascua, M.A., Masana, E., Perea, H., Martín-González, F., Giner-Robles, J., et al., 2012, The Quaternary Active Faults Database of Iberia (QAFI v.2.0): Journal of Iberian Geology, v. 38, no. 1, p. 285–302, doi: 10.5209/rev_JIGE.2012.v38.n1.39219.

Gaspar-Escribano, J.M., Garcia-Castellanos, D., Roca, E., and Cloetingh, S., 2004, Cenozoic vertical motions of the Catalan Coastal Ranges (NE Spain): The role of tectonics, isostasy, and surface transport: Tectonics, v. 23, no. 1, p. TC1004, doi: 10.1029/2003TC001511.

Giménez, J., 2001, Cuantificación de deformaciones recientes en el este de la Península

Ibérica mediante la comparación de datos de ni velación de precisión: Acta Geológica Hispánica, v. 36, p. 21–51.

Giménez, J., Suriñach, E., Fleta, J., and Goula, X., 1996, Recent vertical movements from high-precision leveling data in northeast Spain: Tectonophysics, v. 263, no. 1–4, p. 149–161, doi: 10.1016/S0040-1951(96)00037-6.

Goula, X., Olivera, C., Fleta, J., Grellet, B., Lindo, R., Rivera, L., Cisternas, A., and Carbon, D., 1999, Present and recent stress regime in the eastern part of the Pyrenees: Tectonophysics, v. 308, p. 487–502.

Herraiz, M., De Vicente, G., Lindo-Ñaupari, R., Giner, J., Simón, J.L., González-Casado, J.M., Vadillo, O., Rodriguez-Pascua, M.A., Cicuéndez, J.I., Casas, A., Cabañas, L., Rincón, P., Cortés, A.L., Ramírez, M., et al., 2000, The recent (upper Miocene to Quaternary) and present tectonic stress distribution in the Iberian Peninsula: Tectonics, v. 19, no. 4, p. 762–786.

IGME (1994): Mapa geológico de España. E. 1:1,000,000. IGME, Madrid.

Masana, E., 1995, L’activitat neotectònica a les Cadenes Costaneres Catalanes [PhD Thesis]: Universitat de Barcelona, 444 p.

Masana, E., Villamarín, J.A., Sánchez-Cabañero, J.G., Plaza, J., and Santanach, P., 2001a, Seismogenic faulting in an area of low seismic activity: Paleoseismicity of the El Camp fault (Northeast Spain): Netherlands Journal of Geosciences / Geologie en Mijnbouw, v. 80, no. 3–4, p. 229–241.

Masana, E., Villamarín, J.A., and Santanach, P., 2001b, Paleoseismic results from multiple trenching analysis along a silent fault: The El Camp fault (Tarragona, northeastern Iberian Peninsula): Acta Geológica Hispánica, v. 36, no. 3–4, p. 329–354.

Medialdea, J., Maldonado, A., Alonso, B., Díaz, J.I., Farrán, M., Giró, S., Vázquez, A., Sainz-Amor, E., Martínez, A., and Medialdea, T., 1986, Mapa geológico de la plataforma continental española y zonas adyacentes. Escala 1:200000. Tortosa-Tarragona: , no. 41–42, p. 78.

Olivera, C., Redondo, E., Lambert, J., Riera Melis, A., and Roca, A., 2006, Els terratremols dels segles XIV i XV a Catalunya: Institut Cartogràfic de Catalunya, Barcelona.

Perea, H., 2006, Falles actives i perillositat sísmica al marge nord-occidental dels solc de València: Universitat de Barcelona, 382 p.

Perea, H., 2009, The Catalan seismic crisis (1427 and 1428; NE Iberian Peninsula): Geological sources and earthquake triggering: Journal of Geodynamics, v. 47, no. 5, p. 259–270, doi: 10.1016/j.jog.2009.01.002.

Perea, H., Figueiredo, P.M., Carner, J., Gambini, S., Boydell, K., Berryman, K., Duman, T.Y., Feghhi, K., Ferry, M., Fontana, A., Gountromichou, C., Hus, R., Insua, J.M., Julià, R., et al., 2003, Paleoseismological data from a new trench across the El Camp Fault ( Catalan Coastal Ranges , NE Iberian Peninsula ): Annals of Geophysics, v. 46, no. 5, p. 763–774.

Perea, H., Masana, E., and Santanach, P., 2006, A Pragmatic Approach to Seismic Parameters in a region with Low Seismicity: The Case of Eastern Iberia: Natural Hazards, v. 39, no. 3, p. 451–477, doi: 10.1007/s11069-006-0013-y.

Perea, H., Masana, E., and Santanach, P., 2012, An active zone characterized by slow normal faults, the northwestern margin of the València trough (NE Iberia): a review: Journal of Iberian Geology, v. 38, no. 1, p. 31–52, doi: 10.5209/rev_JIGE.2012.v38.n1.39204.

Roca, E., 1992, L'estructura de la conca Catalano-Balear: paper de la compressió i de la distensió en la seva gènesi [Thesis]: Universitat de Barcelona, 330 p.

Roca, E., 1994, La evolución geodinámica de la Cuenca Catalano-Balear y áreas adyacentes desde el Mesozoico hasta la actualidad: Acta Geol.Hispánica, v. 29, no. 1, p. 3–25.

Roca, E., 2001, The northwestern mediterranean basin (Valencia trough, Gulf of Lions and Liguro-Provençal basins): Structure and geodynamic evolution, *in* Ziegler, P.A., Cavazza, W., Robertson, A.H.F., and Crasquin-Soleau, S. eds., Peri-Tethys Memoir 6: Pery-Tethyan Rift/Wrench Basins and Passive Margins, Mémoires Muséum National d'Histore Naturelle, p. 671–706.

Roca, E., 2004, Estructura, estratigrafía y evolución tectonosedimentaría de las cuencas neógenas de la Cerdanya y Seu d'Urgell (Pirineos orientales), *in* Vera, J.A. ed., SGE-IGME, Madrid, p. 573–576.

Roca, E., and Guimerà, J., 1992, The Neogene structure of the eastern Iberian margin:

Structural constraints on the crustal evolution of the Valencia trough (western Mediterranean): Tectonophysics, v. 203, no. 1–4, p. 203–218, doi: 10.1016/0040-1951(92)90224-T.

Roca, E., Sans, M., Cabrera, L., and Marzo, M., 1999, Oligocene to Middle Miocene evolution of the central Catalan margin (northwestern Mediterranean) (E. Álvarez de Buergo, R. Marten, L. Villalobos, & J. Varela, Eds.): Tectonophysics, v. 315, no. 1–4, p. 209–229, doi: 10.1016/S0040-1951(99)00289-9.

Sàbat, F., Roca, E., Muñoz, J.A., Vergés, J., Santanach, P., Sans, M., Masana, E., Estévez, A., and Santisteban, C., 1995, Role of extension and compression in the evolution of the eastern margin of Iberia: the ESCI-Valencia Trough seismic profile: Revista de la Sociedad Geológica de España, v. 8, no. 4, p. 431–448.

Santanach, P., Masana, E., and Perea, H., 2010, The El Camp fault revisited: 300 ka long paleoseismic history of a slow-slip normal fault in northeastern Iberia, *in* Insua-Arévalo, J.M. and Martín-González, F. eds., Contribución de la geología al análisis de la peligrosidad sísmica, p. 23–26.

Saula, E., Picart, J., Mató, E., Llenas, M., Losantos, M., Berástegui, X., and Agustí, J., 1996, Evolución geodinámica de la fosa del Empordà y las Sierras Transversales: Acta Geol.Hispánica, v. 29, no. 2–4 (1994), p. 55–75.

Schindler, A., Jurado, M.J., and Müller, B., 1998, Stress orientation and tectonic regime in the northwestern Valencia Trough from borehole data: Tectonophysics, v. 300, p. 63–77.

Simón, J.L., 1984, Compresión y distensión alpinas en la cadena ibérica oriental: Universidad de Zaragoza. Publ. Instituto de Estudios Turolenses, 269 p.

Simón, J.L., Arlegui, L.E., Lafuente, P., and Liesa, C.L., 2012, Active extensional faults in the central-eastern Iberian Chain, Spain: Journal of Iberian Geology, v. 38, no. 1, p. 127–144, doi: 10.5209/rev_JIGE.2012.v38.n1.39209.

Simón, J.L., Pérez Cueva, A.J., and Calvo-Cases, A., 1983, Morfogénesis i neotectónica en el sistema de fosas del Maestrat (Provincia de Castellón): Estudios Geológicos, v. 39, p. 167–177.

Simón, J.L., Pérez-Cueva, A.J., and Calvo-Cases, A., 2013, Tectonic beheading of fluvial valleys in the Maestrat grabens (eastern Spain): Insights into slip rates of Pleistocene extensional faults: Tectonophysics, v. 593, p. 73–84, doi: 10.1016/j.tecto.2013.02.026.

Stirling, M., 2002, Comparison of Earthquake Scaling Relations Derived from Data of the Instrumental and Preinstrumental Era: Bulletin of the Seismological Society of America, v. 92, no. 2, p. 812–830, doi: 10.1785/0120000221.

Tassone, A., Roca, E., Muñoz, J.A., Cabrera, L., and Canals, M., 1994, Evolución del sector septentrional del margen continental catalán durante el Cenozoico: Acta Geológica Hispánica, v. 29, no. 2–4, p. 3–37.

Vergés, J., and Sabat, F., 1999, Constraints on the Neogene Mediterranean kinematic evolution along a 1000 km transect from Iberia to Africa (B. Durand, L. Jolivet, F. Horváth, & M. Séranne, Eds.): Geological Society, London, Special Publications, v. 156, no. 1, p. 63–80, doi: 10.1144/GSL.SP.1999.156.01.05.

Vidal, N., Gallart, J., and Danobeitia, J.J., 1995, Contribution of the ESCI-Valéncia Trough Wide-Angle Data to a Crustal Transect in the NE Iberian Margin: Revista de la Sociedad Geologica de España, v. 8, no. 4, p. 417–429.

Villamarín, J.A., Masana, E., Calderón, T., Julià, R., and Santanach, P., 1999, Abanicos aluviales cuaternarios del Baix Camp (provincia de Tarragona): resultados de dataciones radiométricas: Geogaceta, v. 25, p. 211–214.

Wells, D.L., and Coppersmith, K.J., 1994, New empirical relationships among magnitude, rupture length, rupture area and surface displacement: Bull.Seismol.Soc.A., v. 84, p. 974–1002.

Wesnousky, S.G., 1986, Earthquakes, quaternary faults and seismic hazard in California: Journal of Geophysical Research, v. 91 (B12), p. 12587–12631.

Wesnousky, S.G., 2008, Displacement and Geometrical Characteristics of Earthquake Surface Ruptures: Issues and Implications for Seismic-Hazard Analysis and the Process of Earthquake Rupture: Bulletin of the Seismological Society of America, v. 98, no. 4, p. 1609–1632, doi: 10.1785/0120070111.

Zarroca, M., Linares, R., Bach, J., Roqué, C., Moreno, V., Font, L., and Baixeras, C., 2010, Integración de datos geofísicos y de medidas de gases en suelos como herramienta para la caracterización de una falla activa: El ejemplo de Amer (Pirineos, España), *in* Insua-Arévalo, J.M. and Martín-González, F. eds.,

https://doi.org/10.1007/978-3-030-10931-8

Contribución de la geología al análisis de la peligrosidad sísmica, IGME, Sigüenza, Guadalajara, p. 27–30.

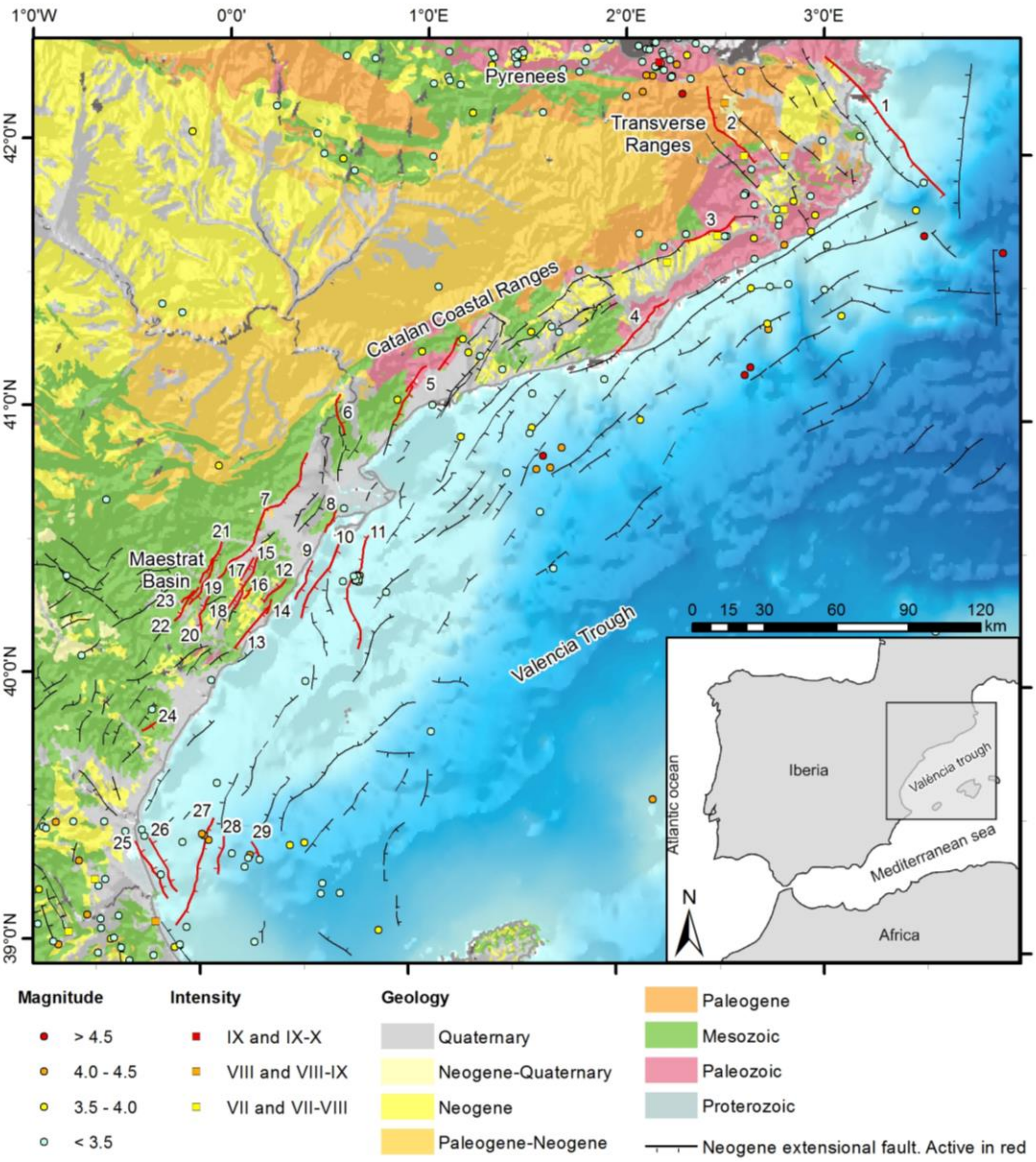


**Figure 1.** Simplified geological map of the northeastern Iberian Peninsula (modified from IGME, 1994), showing the location of the identified Quaternary active fault (in red) and the Neogene extensional faults (in black) (Roca, 1992; Roca and Guimerà, 1992), and the historical (I > VII) and instrumental seismicity reported by the Instituto Geográfico Nacional earthquake catalog. Quaternary active faults: 1. Gulf of Roses; 2. Amer; 3. Montseny; 4. Pla de Barcelona; 5. El Camp; 6. Pla de Burgar; 7. Baix Ebre; 8. Montsià; 9. Western Amposta basin; 10. Central Amposta basin; 11. Eastern Amposta basin; 12. Alcalà de Xivert; 13. Torreblanca; 14. Irta range; 15. Salzedella; 16. Val d'Àngel; 17. La Vall Torta/Mas de Calduchs; 18. Torre Endomenech/Vall d'Alba; 19. Albocàsser; 20. Ivarsos/Rambla de la Viuda; 21. Catí; 22. Eastern Atzeneta; 23. Western Atzeneta; 24. Vall d'Uixó; 25. Western Cullera cape; 26. Central-western Cullera cape; 27. Central-eastern Cullera cape; 28. Eastern Cullera cape; 29. SW Columbrets basin. The seismogenic parameters of the numbered Quaternary active faults are given in Table 1.

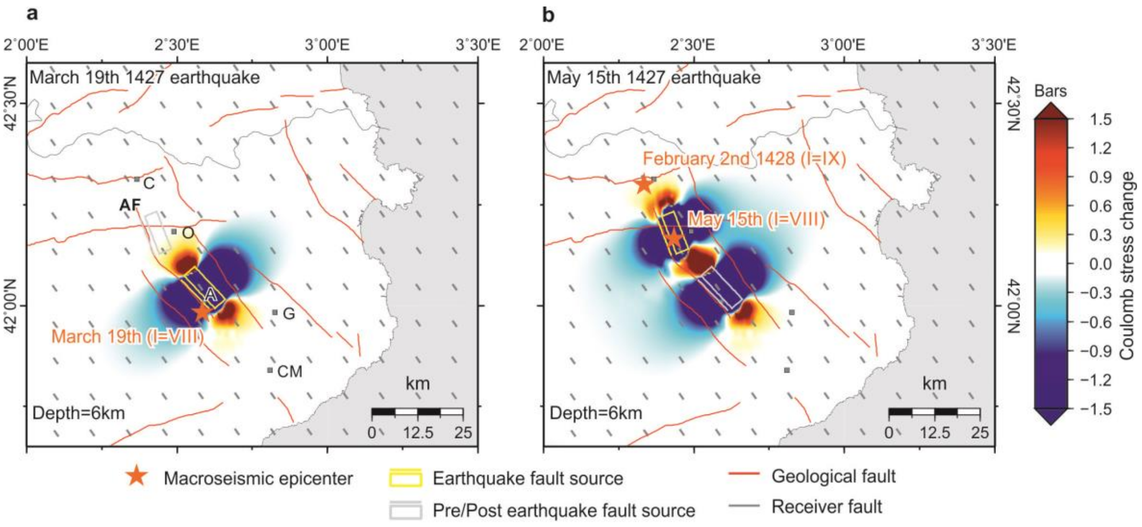


**Figure 2.** Maps showing the Coulomb failure stress change at 6km depth in different periods of the Catalan seismic crisis (modified from Perea, 2009). (a) Map with the location of the March 19th 1427 earthquake macroseismic epicenter and the Coulomb failure stress change distribution. (b) Map with the location of the May 15th 1427 and February 2nd 1428 earthquakes macroseismic epicenters and the Coulomb stress change distribution corresponding to the occurrence of the March and May events. Cities/towns: A: Amer; C: Camprodon; CM: Caldes de Malavella; G: Girona; O: Olot. AF: Amer fault.

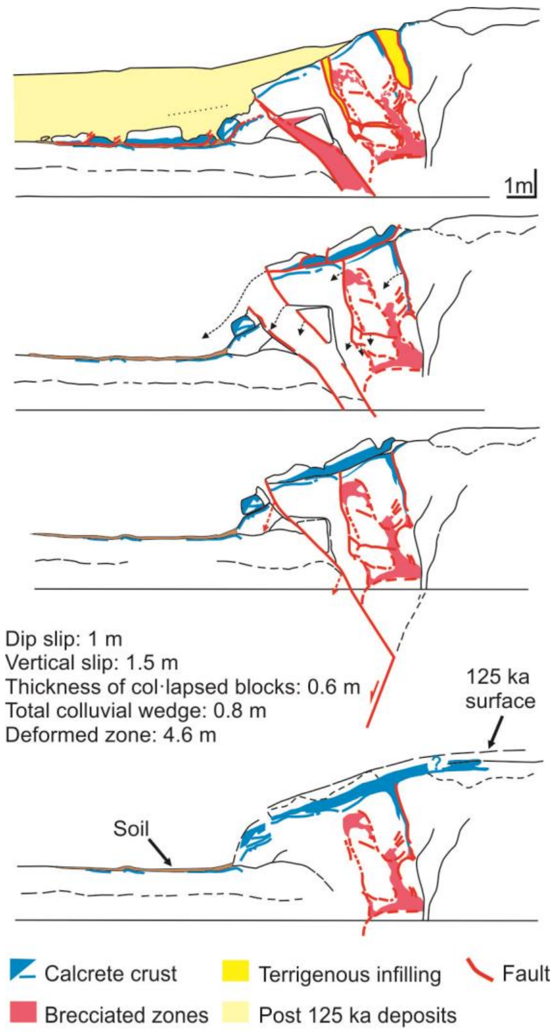


**Figure 3.** Restoration of the deformation related to the seismic event that caused a coluvial wedge in trench 4 on El Camp fault and calculated slip values of the event (modified from Santanach et al., 2010).

## Table Captions

| Fault | Fault length (km) | Fault max. magnitude (Mw)[a] | Fault vertical slip rate (mm/yr)[b] | Fault net slip rate (mm/yr)[c] | Fault recurrence interval (years)[c] (range in brackets) |
|---|---|---|---|---|---|
| 1. Gulf of Roses | 76,0 | 7.0-7.3 | 0,03-0,07 | 0,04-0,08 | 64618 (7779-231929) |
| 2. Amer | 35,4 | 6.8-6.9 | 0,05-0,14 | 0,05-0,16 | 25540 (2864-112823) |
| 3. Montseny | 23,1 | 6.7-6.8 | 0,04-0,11 | 0,05-0,13 | 26219 (2945-94105) |
| 4. Pla de Barcelona | 25,0 | 6.7-6.8 | 0,02-0,04 | 0,02-0,04 | 52216 (9919-330731) |
| 5. El Camp | 41,1 | 6.9-7.0 | 0,02-0,06 | 0,02-0,09 | 75723 (5275-271786) |
| 6. Pla de Burgar | 17,0 | 6.5-6.7 | 0,02-0,05 | 0,02-0,05 | 41258 (6426-204993) |
| 7. Baix Ebre | 80,0 | 7.0-7.4 | 0,04-0,11 | 0,03-0,13 | 44454 (5071-162864) |
| 8. Montsià | 11,0 | 6.2-6.4 | 0,03-0,09 | 0,04-0,09 | 24867 (3079-99168) |
| 9. Western Amposta basin | 18,0 | 6.5-6.7 | 0,01-0,03 | 0,01-0,04 | 53314 (9761-366766) |
| 10. Central Amposta basin | 35,0 | 6.8-6.9 | 0,01-0,03 | 0,01-0,04 | 70725 (12949-486542) |
| 11. Eastern Amposta basin | 16,0 | 6.4-6.7 | 0,08-0,13 | 0,16-0,26 | 14430 (3247-67976) |
| 12. Alcalà de Xivert | 14,5 | 6.4-6.6 | 0,03-0,07 | 0,03-0,08 | 31959 (3945-129509) |
| 13. Torreblanca | 30,0 | 6.8-6.9 | 0.04-0.30 | 0.05-0.35 | 4555 (1195-17428) |
| 14. Irta range | 5,9 | 5.9-6.2 | 0,02-0,06 | 0,03-0,06 | 21809 (3323-109586) |
| 15. Salzedella | 23,5 | 6.7-6.8 | 0,02-0,04 | 0,02-0,05 | 59710 (7653-246461) |
| 16. Vall d'Àngel | 8,5 | 6.1-6.3 | 0,02-0,05 | 0,02-0,06 | 25583 (3564-115778) |
| 17. La Vall Torta/Mas de Calduchs | 6,7 | 6.0-6.2 | 0.02-0.04 | 0.02-0.05 | 22197 (4810-111539) |
| 18. Torre Endomenech/Vall d'Alba | 26,0 | 6.7-6.8 | 0.02-0.04 | 0.02-0.05 | 60106 (11672-381683) |
| 19. Albocàsser | 20,4 | 6.6-6.7 | 0,05-0,14 | 0,06-0,14 | 22297 (2592-84394) |
| 20. Ivarsos/Rambla de la Viuda | 15,2 | 6.4-6.7 | 0,05-0,18 | 0,05-0,21 | 34594 (3954-128170) |
| 21. Catí | 20,0 | 6.5-6.7 | 0,05-0,11 | 0,05-0,13 | 24129 (2689-86605) |
| 22. Eastern Atzeneta | 18,0 | 6.5-6.7 | 0,04-0,09 | 0,04-0,10 | 30656 (3486-112851) |
| 23. WesternAtzeneta | 9,5 | 6.2-6.4 | 0,03-0,07 | 0,03-0,08 | 26702 (3472-111812) |
| 24. Vall d'Uixó | 6,6 | 5.9-6.2 | 0,01-0,03 | 0,01-0,03 | 36534 (6161-201062) |
| 25. Western Cullera cape | 28,0 | 6,8 | 0,02-0,05 | 0,02-0,06 | 42271 (7107-230880) |
| 26. Central-west. Cullera cape | 25,0 | 6.7-6.8 | 0,03-0,08 | 0,04-0,09 | 40284 (4270-144588) |
| 27. Central-east. Cullera cape | 48,0 | 6.9-7.1 | 0,01-0,03 | 0,01-0,04 | 62013 (14809-556442) |
| 28. Eastern Cullera cape | 16,0 | 6.4-6.7 | 0,01-0,02 | 0,01-0,02 | 50710 (14128-348849) |
| 29. SW Columbrets basin | 10,0 | 6.2-6.4 | 0,01-0,03 | 0,01-0,04 | 41530 (11571-285698) |

a. Magnitude range calculated using the empirical relationships on Sterling (2002), Wells and Coppersmith (1994) and Wesnousky (2008). The last one just used for faults larger than 15 km.

b. Data from García-Mayordomo et al. (2012), Perea (2006), Perea et al. (2006; 2012) and Simón et al. (2012; 2013)

c. Data from García-Mayordomo et al. (2012)

**Table 1.** Seismic parameters corresponding to the active faults located in the northeastern margin of the Iberian Peninsula (Perea, 2006; Perea et al., 2006, 2012; García-Mayordomo et al., 2012; Simón et al., 2012, 2013). The fault maximum magnitude range has been calculated using different empirical relationships (Wells and Coppersmith, 1994; Stirling, 2002; Wesnousky, 2008), for normal faults when possible, and considering the fault map length as the maximum surface rupture length and the valid ranges for each relationship. The fault recurrence interval range has been calculated using the relationship in Wesnousky (1986).The geographical location of the faults, identified by the same numbers, is given in Figure 1.